

Planar Resistors for Probe Station Calibration¹

D.K. Walker, D.F. Williams, and J. M. Morgan
National Institute of Standards and Technology
Boulder, Colorado

Abstract

This paper investigates the effects of variations in sheet resistance, geometry, distance from the probe tip, and fabrication processes on the impedance of planar nickel-chromium resistors. Resistor reactance is a strong function of film resistance, but depends only weakly on geometry and distance from the probe tip. Photoresist contamination in the resistive film induces more complicated impedance behavior, even at low frequencies. The impact on circuit design and time- and frequency-domain calibrations is considered in light of these results.

Introduction

In this work, we investigate the electromagnetic behavior of planar nickel-chromium (Ni-Cr) resistors terminating coplanar waveguide (CPW) transmission lines. The impedance of these resistors is usually assumed to be real, constant, and equal to its dc resistance. While planar resistors are commonly used for circuit design, network-analyzer calibration, and time-domain reflectometer normalization, the commonly-employed assumptions concerning resistor impedance have not been systematically investigated, to the best of our knowledge. Here we investigate these assumptions in carefully controlled experiments. We show resistor reactance to be a strong function of film sheet resistance, but to depend only weakly on geometry and distance from the probe tip. Photoresist contamination between the gold contacts and the resistive Ni-Cr film induces more complicated impedance behavior at frequencies down to 100 MHz or less. Also, in some on-wafer calibrations, the resistor is placed close to the probe tip, and the interaction of the probe tip and the resistor must be considered as well. We show that the resistor and the probe tip do not interact significantly.

Resistor Impedance

We fabricated resistors by thermally evaporating approximately 20 nm of Ni-Cr with a nominal composition of 80% nickel and 20% chromium by weight onto a gallium arsenide (GaAs) substrate through a photoresist mask. We then embedded the patterned resistors in CPW lines formed by evaporating 1 μm of gold through a second photoresist mask, as illustrated in

¹ Publication of the National Institute of Standards and Technology, not subject to copyright.

Figure 1a. The CPW lines consisted of a 73 μm wide signal line separated from two 250 μm wide ground planes by 49 μm gaps. The resistors were annealed at 300°C in air for 30 min to stabilize the film.

We determined the resistor impedance, Z , by applying a Thru-Reflect-Line (TRL) calibration [1]. We determined the characteristic impedance of the CPW lines from the capacitance per unit length of the lines, which was assumed constant, as explained in [2] and [3], and set the measurement reference plane at the leading edge of the rectangular resistors and the reference impedance of the calibration to 50 Ω .

We found resistor impedance as a function of frequency to be characterized by a roughly constant real part equal to the resistor's dc resistance and a linearly increasing or decreasing reactance. To quantify the resistor reactance from the measured resistor impedance we determined what we will call its effective inductance, L_e , defined by

$$L_e = \frac{\sum_f \frac{\text{Im}(Z)}{2\pi f} \cdot f}{\sum_f f}, \quad (1)$$

where the frequencies f in the sums run from 2 GHz to 40 GHz. L_e is, in essence, a weighted estimate of the resistor's series inductance. L_e does, however, take on negative values when the slope of the imaginary part of the resistor reactance with respect to frequency is negative, and thus does not correspond to a physical inductance.

We plotted L_e for our nominally 73 μm wide by 67 μm long resistors as a function of their dc resistance in Figure 2. These data reveal a surprisingly large range of effective inductance which depends strongly on resistor dc resistance. The different symbols correspond to the distance between the beginning of the CPW line and the beginning of the resistor. The probe tip overlaps the CPW line by about 50 μm , so the distance between the probe tip and the resistor is somewhat less than the distances indicated in the figure. The data indicate that the probes do not interact significantly with the resistors, even when the resistors are only about 25 μm in front of the probe tip.

It has been suggested that perhaps the observed variation in reactance with dc resistance may be related to the electromagnetic characteristics of the CPW line in which the resistors are embedded. In order to investigate this possibility, we developed the simple electrical model of Figure 1b for the section of CPW line in the vicinity of the resistor. The parameters labeled C and L in the model are assumed to be the capacitance of the resulting gap when the resistor is removed, and the inductance of the line and offset short when the dc resistance of the resistor goes to zero, respectively. Measurements of an open (Figure 1b) and an offset short (Figure 1c) were made with respect to the TRL calibration to determine the values $C = 7.7$ fF and $L = 0.044$ nH for 73 μm by 73 μm resistors. For our 73 μm by 67 μm resistors which, due to

overexposure of the photoresist, were actually located approximately $3 \mu\text{m}$ in front of the measurement reference plane, we obtained $C = 8.3 \text{ fF}$ and $L = 0.043 \text{ nH}$. Because the reactance of the equivalent circuit model of Figure 2 is linear at low frequencies, it is possible to determine an effective inductance for the model, which, with a simple linear analysis, is given by $L - CR^2$. We plotted $L - CR^2$ for our $73 \mu\text{m}$ by $67 \mu\text{m}$ resistor model alongside the measured data in Figure 2 for comparison. The fit to the data is surprisingly good.

We also investigated the dependence of L_e on resistor geometry. In Figure 3 we have plotted L_e for resistors of varying geometry alongside the data of Figure 2. The measurement reference plane was $275 \mu\text{m}$ from the end of the CPW line in all cases. While we would not expect our simple model to be valid except for our nominally $73 \mu\text{m}$ wide by $67 \mu\text{m}$ long resistors, we have plotted $L - CR^2$ to emphasize the difference between our nominal resistors and the data for the other resistors shown in the figure. The variation in L_e is again a strong function of dc resistance, but depends only weakly on geometry. The shorter and wider resistors, however, have a slightly lower L_e than predicted by our model, as might be expected from physical arguments.

Small amounts of photoresist residue, common in the chlorobenzene-based photolithographic patterning we used, may also strongly affect resistor impedance. This is illustrated in Figure 4. The resistor on which we detected photoresist residue has a frequency-dependent impedance which contrasts sharply with the constant resistance and linear reactance behavior typically observed for a resistor lacking such residue.

We presumed that the unexpected electrical behavior of the resistors with photoresist residue was caused by a capacitive layer formed by the photoresist between the gold contacts and the resistive Ni-Cr film, as illustrated in Figure 5. Pinholes or other breaks in the residue allow conduction at dc. To investigate the validity of this presumption, we developed the equivalent electrical circuit of Figure 5 and adjusted the values of C_1 , R_1 , R_2 , L_{54} , and R until a good fit to the data was achieved. The total resistance $R + R_1 + R_2$ was held equal to the measured dc resistance during the fit. The resulting impedance is plotted as a solid curve alongside the data in Figure 4. The good fit to the data is an indication, at least, that the photoresist residue between the gold contacts and the resistive nichrome film greatly affects the electrical behavior. The asymmetrical nature of the circuit is indicative of the high local variability in the thickness of the photoresist residue, which was confirmed qualitatively by microscopic analysis using dark-field illumination.

Conclusion

These results have several ramifications for the design of MMICs and for the calibration of network-analyzers and time-domain reflectometers. Foremost among these is that thin film resistors have a significant reactance which depends strongly on their dc resistance. Fortunately, the mechanism by which the inductance of the resistors varies with dc resistance appears to be due largely to the electromagnetic characteristics of the embedding transmission line, simplifying modeling and allowing an approximate prediction of reactance based on a simple equivalent

circuit. Thus it should be straightforward to modify resistor models in computer-aided design tools used for circuit design, to transform the reference impedance of some network-analyzer calibrations based on lumped elements to some desired value, usually $50\ \Omega$, and to perform time-domain reflectometer normalizations with imperfect but well-characterized shorted and matched elements when gating is used to avoid receiving unwanted secondary reflections.

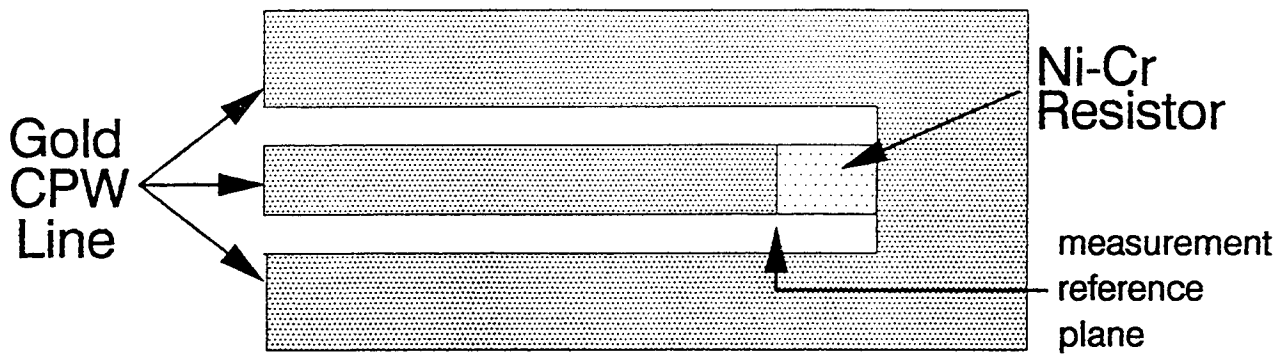
The presence or absence of photoresist residue in our chlorobenzene-based liftoff process depends upon relatively small (and seemingly innocuous) process variations, such as temperature or relative humidity fluctuations in the processing area. This makes photoresist contamination difficult to control in chlorobenzene liftoff. Furthermore, the small quantities of photoresist residue in our devices were often difficult to detect with standard bright- or dark-field microscopy. Thus it seems prudent to measure resistor impedance over the frequency range of interest when photoresist contamination is possible.

Acknowledgement

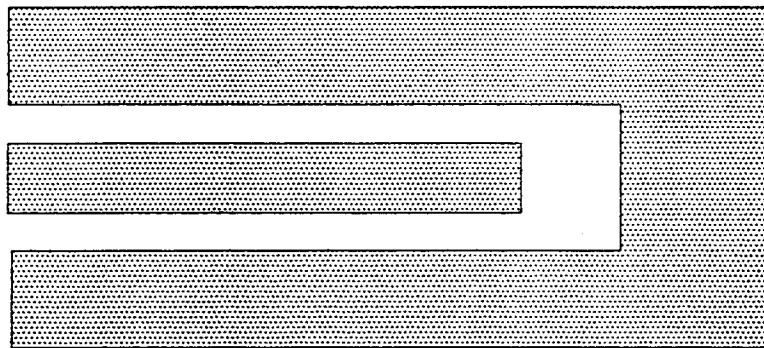
The authors would like to thank Mr. Reed Gleason at Cascade Microtech, Inc., for suggesting the resistor-embedding structure equivalent-circuit model discussed in this work.

References

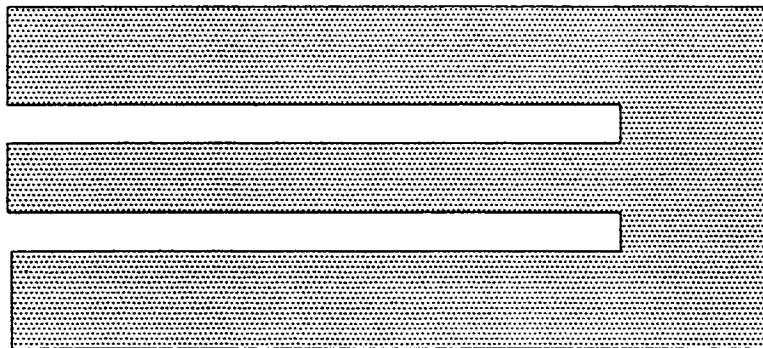
1. G. F. Engen and C. A. Hoer, "Thru-Reflect-Line: An Improved Technique for Calibrating the Six-Port Automatic Network Analyzer," *IEEE Trans. Microwave Theory Tech.*, vol. MTT-27, pp. 987-993, Dec. 1979.
2. R. B. Marks and D. F. Williams, "Characteristic Impedance Determination Using Propagation Constant Measurement," *IEEE Microwave and Guided Wave Letters*, Vol. 1, No. 6, pp. 141-143, June 1991.
3. D. F. Williams and R. B. Marks, "Transmission Line Capacitance Measurement," *IEEE Microwave and Guided Wave Letters*, Vol. 1, No. 9, pp. 243-245, Sept. 1991.



a. RESISTOR TEST STRUCTURE



b. CAPACITANCE TEST STRUCTURE



c. INDUCTANCE TEST STRUCTURE

Figure 1. Geometry of the test structures. The resistor geometry is shown in a and the test structures used to determine the values of C and L shown in b and c respectively. The resistor equivalent circuit model is shown in the upper right of Figure 2.

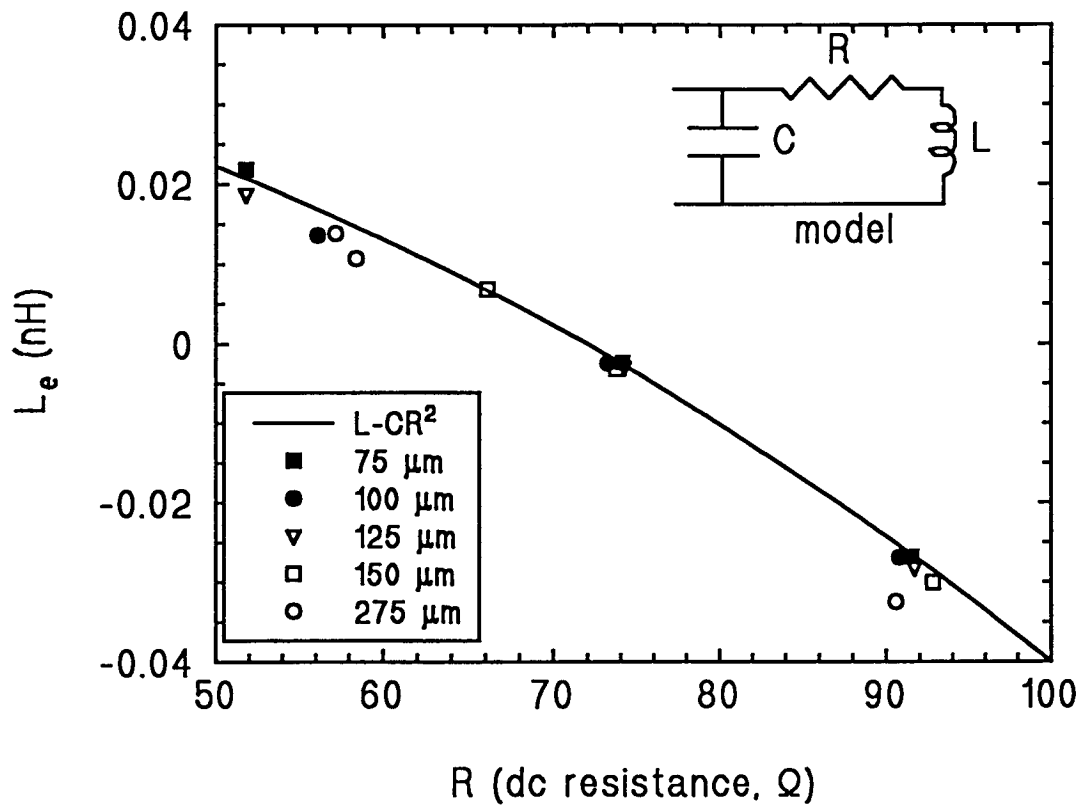


Figure 2. L_e as a function of the dc resistance for our nominal nichrome resistors. The different symbols correspond to the distance between the beginning of the CPW line and the beginning of the resistor. The probe tip overlaps the CPW line by about $50 \mu\text{m}$. The solid curve represents $L - CR^2$ for the model described in the text and shown in the upper right of the figure.

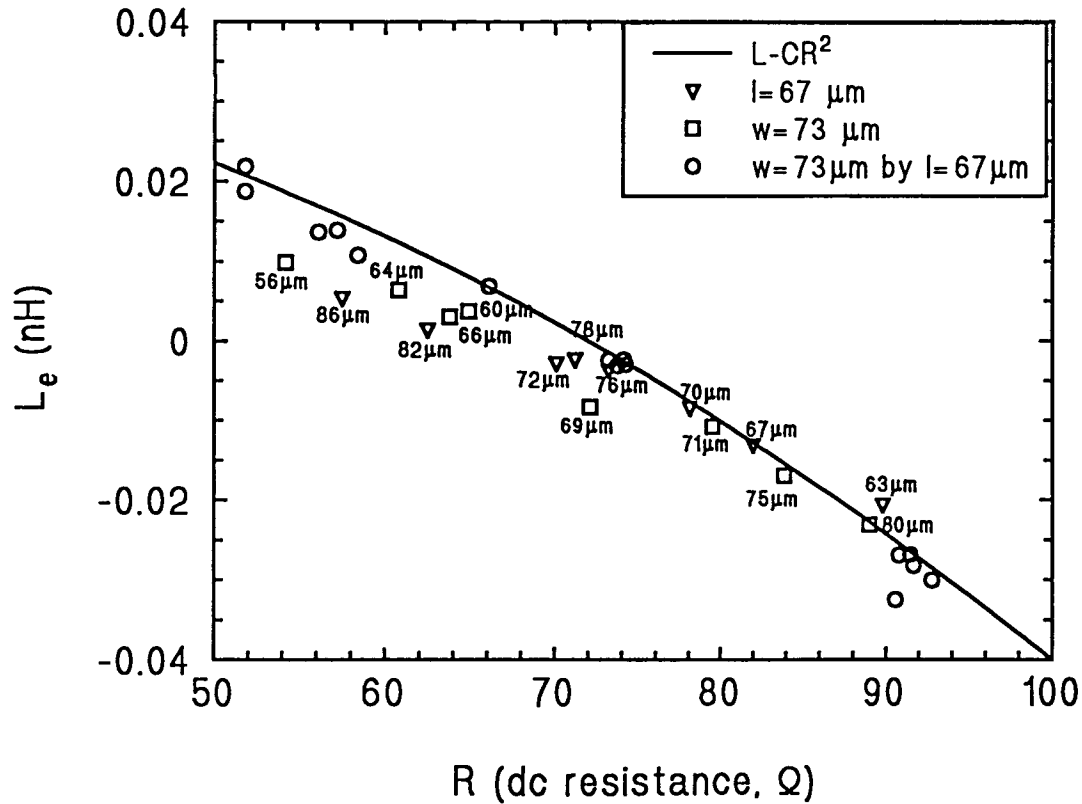


Figure 3. L_e as a function of dc resistance for resistors of varying length and width. $73\ \mu\text{m}$ by $67\ \mu\text{m}$ resistors are represented by circles. Resistors of width $73\ \mu\text{m}$ are represented by squares and the resistor length is printed next to the data point. Resistors of length $67\ \mu\text{m}$ are represented by triangles and the resistor width is printed next to the data point. The solid curve represents $L-CR^2$ for the model described in the text and shown in the upper right of the Figure 2.

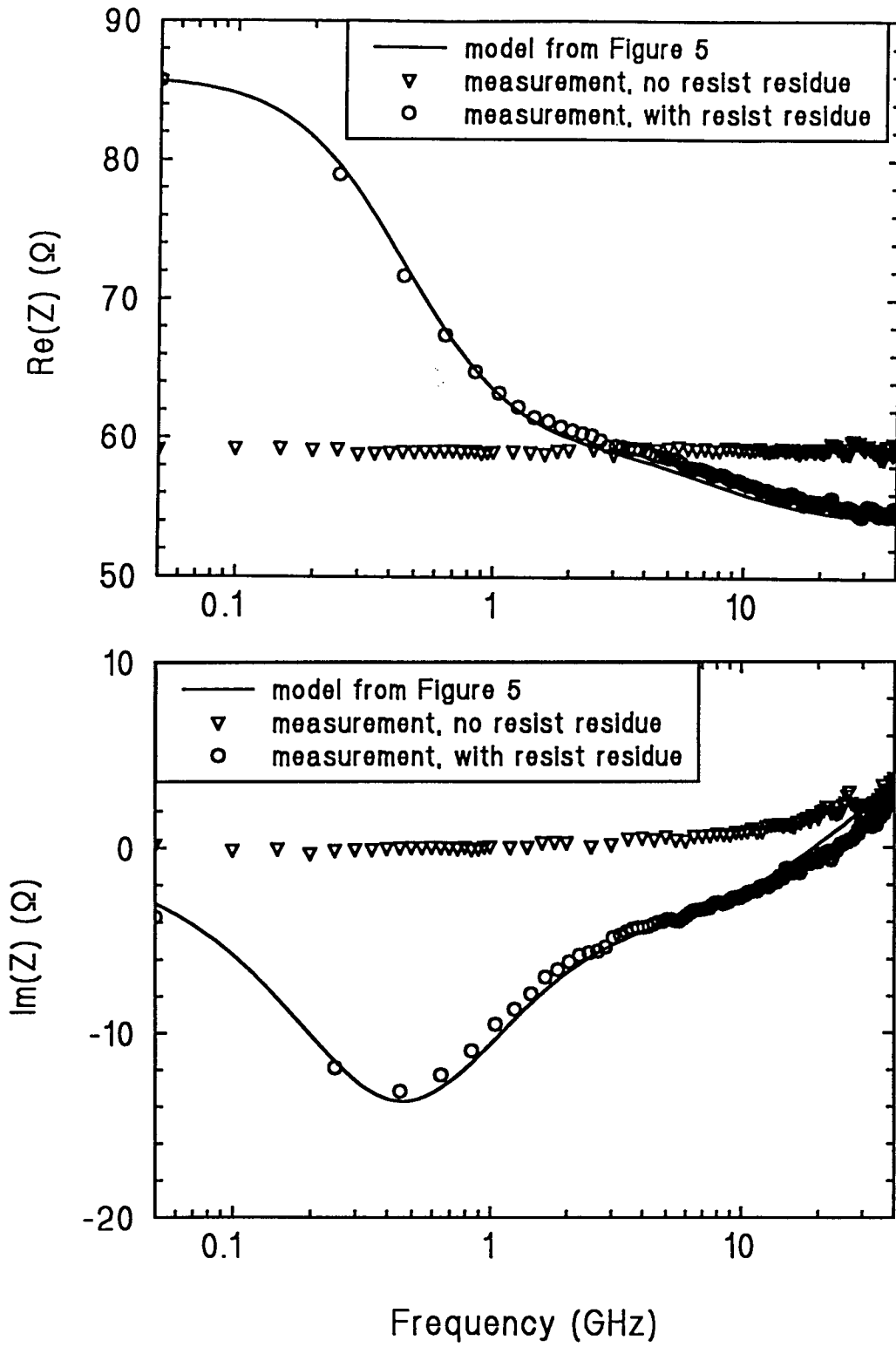
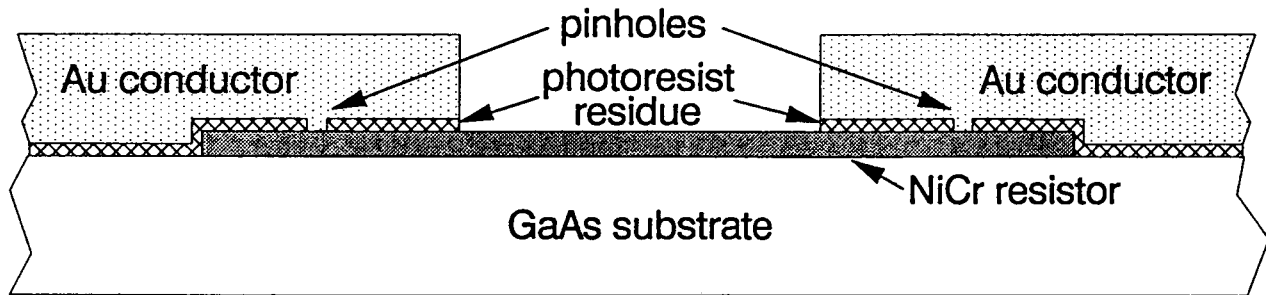
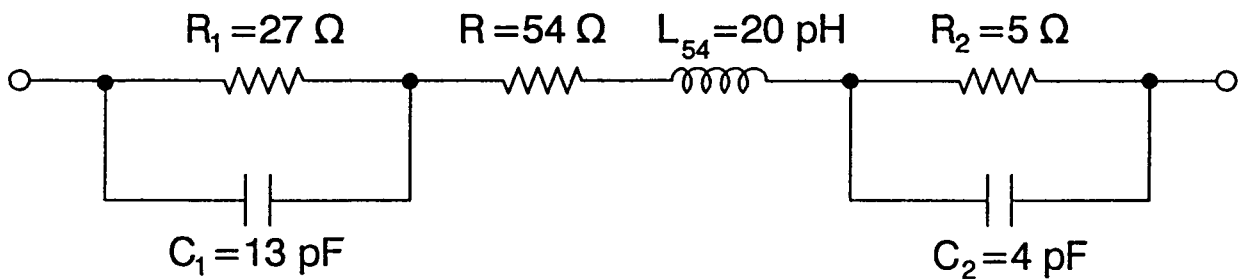


Figure 4. Real and imaginary parts of the impedance, Z , for resistors with and without photoresist residue contamination as a function of frequency. The solid line represents the impedance of the equivalent circuit of Figure 5.



PHYSICAL MODEL



ELECTRICAL MODEL

Figure 5. Physical and electrical resistor models with photoresist residue. Photoresist residue is presumed to form a capacitive layer between the gold conductors and the resistive nichrome film. Pinholes or other breaks in the photoresist residue are assumed to form dc connections to the nichrome film.